Quantitative description of C_{60} diffusion on an insulating surface

Felix Loske,[1] Jannis Lübbe,[2] Jens Schütte,[1] Michael Reichling,[2] and Angelika Kühnle[1,*]

[1]*Institut für Physikalische Chemie, Johannes Gutenberg-Universität Mainz, Jakob-Welder-Weg 11, 55099 Mainz, Germany*
[2]*Fachbereich Physik, Universität Osnabrück, Barbarastraße 7, 49076 Osnabrück, Germany*

The diffusion of C_{60} molecules on large, atomically flat terraces of the $CaF_2(111)$ surface is studied under ultrahigh vacuum conditions at various substrate temperatures below room temperature. The weak molecule-substrate interaction on this insulating surface makes a direct observation of hopping events difficult. Therefore, to determine a quantitative value of the diffusion barrier, we employ the so-called onset method. This method is based on the analysis of spatial properties of islands created by nucleation of diffusing C_{60} molecules, as measured by noncontact atomic force microscopy. We first determine the critical cluster size to be $i^* = 1$ from coverage-dependent island size distributions prepared at a fixed substrate temperature. The diffusion barrier of $E_d = (214 \pm 16)$ meV and an attempt frequency of $\nu_0 = 1.4 \times 10^{12 \pm 0.6}$ s^{-1} are then obtained by analyzing the island densities at different substrate temperatures.

I. INTRODUCTION

The concept of using organic molecules as building blocks for functional devices has attracted great interest since decades.[1] A versatile strategy for building functional structures is molecular self-assembly.[2–4] In particular, a detailed knowledge of both intermolecular as well as molecule-substrate interactions is required to control the growth process for successfully employing self-assembly techniques in device fabrication.[5,6] The most important parameter for the migration of molecules on surfaces is the diffusion barrier and, consequently, several methods have been developed for the experimental determination of the diffusion barrier.[7–9] The vast majority of these studies have, however, been performed using metallic rather than insulating substrates. This is largely due to the fact that most surface science-based analysis methods require conducting substrates. For application in molecular electronics, however, it is most desirable to arrange organic molecules on insulating rather than metallic surfaces in order to decouple the electronic structure of the molecular device from the substrate.

A widely used technique to study adsorbate diffusion is analyzing single hopping events.[6] Using this technique, diffusion has extensively been studied for atomic species on metallic surfaces and results have been reviewed in Refs. 6, 8, and 10–13. Also for organic molecules on metal surfaces, the diffusion parameters were determined by direct observation of hopping events.[6,12,14–16] These studies have revealed diffusion barriers for organic molecules on metallic substrates often being considerably larger than 800 meV, a barrier height that allows for monitoring single adsorbate jumps at room temperature.[6,14,15] For instance, a value of 1400 meV has been found for diffusion of C_{60} on Pd(110).[16]

In general, the diffusion barrier of organic molecules on insulating surfaces is much smaller than on metallic surfaces,[6,17,18] as evidenced by a strong clustering of organic molecules on insulating surfaces.[19–21] Due to the small diffusion barrier, monitoring of individual molecular jumps is, therefore, not feasible at room temperature. Moreover, in the case of small diffusion barriers, a direct observation of single

hopping events may be influenced by the interaction between the imaging tip and the molecule, as observed in scanning tunneling microscopy[22–24] and noncontact atomic force microscopy (NC-AFM) imaging.[25–28]

In cases where a direct observation of single hopping events is not possible, the analysis of island densities at different growth temperatures (so-called *onset method*) has been proven to provide reliable values for the diffusion barrier.[23] Using this technique, the diffusion barrier has been determined for a few molecular systems on metallic and semiconducting surfaces.[29,30] On insulating surfaces, however, quantitative analysis of molecular diffusion has been performed very rarely so far,[31–35] revealing diffusion barriers ranging from 100 to 400 meV.[32,34,35] The latter experiments were, however, not accomplished under ultrahigh vacuum (UHV) conditions in all steps. Such experimental conditions result in an increased surface contamination and may, therefore, alter molecular diffusion and influence the island density and island size distribution.[7]

In this work, we employ the onset method to determine the diffusion barrier and attempt frequency for the tracer diffusion of C_{60} molecules on an insulating and atomically flat surface, namely, $CaF_2(111)$. Our results reveal a diffusion barrier of $E_d = (214 \pm 16)$ meV for this system, much smaller than what is typically observed for C_{60} molecules on metallic surfaces. In contrast to previously described studies of organic molecules on insulating surfaces, our work is performed under UHV conditions, revealing quantitative results that are not affected by surface contaminants.

II. EXPERIMENTAL METHODS

For our experiments, we use cleaved surfaces of high purity CaF_2 crystals (Korth Kristalle, Altenholz, Germany). Prior the experiments, crystals were outgased in UHV for 1.5 h at 425 K. After the sample had cooled down to room temperature, the crystal was cleaved *in situ* and heated again (1.5 h at 425 K) to remove charges trapped on the surface.[36] The cleaved surface reveals atomically flat terraces with dimensions often larger than 4 μm^2 when applying a recently de-
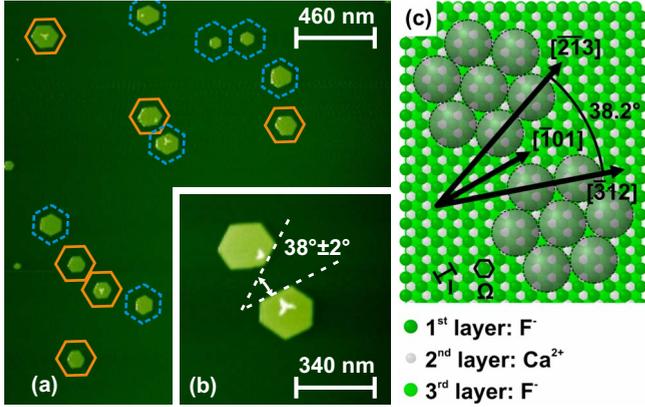
FIG. 1. (Color online) In (a) and (b) NC-AFM images (topography) are shown, prepared at a substrate temperature $T_S=169$ K with subsequent quenching to 92 K. We clearly observe two domains with an angle of $38° \pm 2°$ in between, in good agreement with the value determined in Ref. 40. (c) Model for the two different island types as previously suggested by Fölsch *et al.* (Refs. 40 and 41) using reflection high-energy electron diffraction. The C_{60} molecules arrange in a hexagonal configuration, with a nearest-neighbor distance close to that of a bulk C_{60} crystal. Two different domains exist with close-packed C_{60} directions parallel to the CaF_2 $[2\bar{1}3]$ and $[\bar{3}12]$ direction, respectively. The angle between both domains amounts to 38.2°. Note that the exact adsorption sites remain unknown and that arbitrary positions are chosen in the sketch.

veloped cleavage technique.[37] Directly after the preparation of the bare substrate, the sample was cooled down to a defined substrate temperature between $T_S=96$ K and $T_S=217$ K by a liquid nitrogen flow cryostat thermally coupled to the sample holder. The temperature was adjusted and stabilized by regulating the liquid-nitrogen flow through the cooling plate beneath the sample. Once the desired temperature was stabilized (≈ 0.5 h), the C_{60} molecules (purity of 99.95%, MER Corporation, Tuscon, Arizona) were deposited onto the surface by sublimation from a homemade Knudsen cell heated to 528 K with a deposition rate (flux) of $F=5 \times 10^{-4}$ s^{-1} nm^{-2}. After C_{60} deposition, the sample was quenched to 92 K and transferred into the AFM situated in the same UHV system. Measurements were performed with an RHK 750 variable temperature force microscope (RHK inc., Troy, Michigan, USA) under UHV conditions, using frequency modulation noncontact atomic force microscopy (FM NC-AFM). Results shown in Fig. 1, however, were obtained with an Omicron VT-AFM 25 system (Omicron GmbH, Taunusstein, Germany). Details about the tips and their preparation have been described previously.[38] To minimize long-range electrostatic interactions, an appropriate bias voltage not exceeding ± 10 V was applied to the tip. The compensating voltage was determined via Kelvin probe force spectroscopy.[39] The temperature on the cleaved sample surface differs to the one measured at the cooling plate beneath the sample. Because the temperatures directly on the surface are of interest, the surface temperature was calibrated once with a type K thermocouple directly glued onto the sample surface. We assume an error of $\Delta T_S = \pm 5$ K for the temperature measurement.

III. ADSORPTION GEOMETRY

Figure 1(a) shows an overview image of C_{60} island formation on $CaF_2(111)$ prepared at a substrate temperature of $T_S=169$ K. As can clearly be seen, all islands exhibit an overall hexagonal shape. The orientation of the islands with respect to the substrate reveals a grouping of islands into two different domains as illustrated in Fig. 1(a) by solid red and dashed blue hexagons, respectively. The sides of islands from different domains enclose an angle of $38° \pm 2°$, as shown in Fig. 1(b). In Fig. 1(c) a structural model for the possible arrangement of C_{60} molecules on the atomic lattice is presented that would result in an angle of 38.2° between the two domains. This model is in perfect agreement with previously presented results from Fölsch *et al.*[40,41] who have studied the adsorption of C_{60} on the $CaF_2(111)$ by means of reflection high-energy electron diffraction.

Assuming single jumps of molecules between the adsorption sites defined by this model, we define a single jump length of $l=386$ pm (distance between two adsorption sites). The area of an adsorption site that is a hexagonal unit allowing a space-filling coverage of the surface without overlap amounts to $\Omega = \sqrt{3}/2l^2 = 1.29 \times 10^5$ pm^2 (a single adsorbed C_{60} molecule covers about six adsorption sites). Jump length and adsorption site area are marked in Fig. 1(c).

When preparing islands at substrate temperatures larger than 220 K, C_{60} molecules appear to nucleate in the second layer, however, this will not be discussed here but in a forthcoming publication. The second layer occupation does arise from direct impinging molecules as well as from molecules dewetting from the surface to the second layer.[20] To facilitate an unambiguous island size distribution analysis, care was taken to restrict the present study to single-layer islands. Thus, the present study is limited to substrate temperatures $T_S \leq 220$ K and coverages $\theta \leq 0.28$ ML. In this regime, the islands exhibit only very few C_{60} molecules in the second layer as seen as tiny bright structures on top of islands in Figs. 1(a) and 1(b). At the highest temperature used here (217 K) the second layer occupation is 5% at 0.1 ML and rises to 14% for 0.28 ML. At all lower temperatures, the second layer occupation is smaller than 5% at a coverage of 0.1 ML.

IV. GROWTH MODEL

A. Island density

To determine the diffusion barrier E_d and the attempt frequency ν_0 from island densities, a growth model has to be applied. For obtaining an analytical model describing nucleation and growth upon molecular deposition, some simplifying assumptions are made:[7,8] (a) single molecules are the only mobile species and do not desorb from the surface (*complete condensation*). (b) In addition, a distinction between stable and unstable clusters is made, which implies a *critical island size* i^*. Stable clusters with sizes $a > i^*$ are not allowed to shrink but can further grow by capture of single molecules. Unstable clusters with size $a \leq i^*$ are allowed to decay, i.e., $i^*=1$ implies that dimers and all larger clusters are stable. Note, that the critical cluster size i^* depends on

deposition parameters (such as flux F and substrate temperature T_S during deposition) and is not a constant intrinsic value for the molecules-substrate system.

With these assumptions, the following equation has been derived for the steady state nucleation regime:[7,42–45]

$$\hat{N} = 0.25 \left(\frac{\Omega^2 F}{D} \right)^{i^*/i^*+2} \exp \left(\frac{1}{i^*+2} \frac{E_{i^*}}{k_B T_S} \right), \qquad (1)$$

where $\hat{N}$ is the number of islands per adsorption site, Ω is the area of one adsorption site, F is the molecule flux, k_B is the Boltzmann constant, T_S is the substrate temperature and E_{i^*} is the cluster binding energy gained in forming a cluster of size i^*. A cluster consisting of one molecule has no cluster binding energy, therefore $E_1 = 0$. The diffusion coefficient D in two dimensions is defined by[10]

$$D = \frac{1}{4} l^2 \nu_0 \exp \left(-\frac{E_d}{k_B T_S} \right), \qquad (2)$$

where l is the distance between two adsorption sites covered in a single jump, ν_0 is the attempt frequency and E_d is the diffusion barrier.

Combining Eqs. (1) and (2) allows to reveal the diffusion barrier and the attempt frequency from the so-called *onset experiment*. A short outline of the onset experiment is given in the following. A small amount of atoms/molecules is deposited onto the surface, using a fixed flux F and coverage θ. During deposition, the substrate temperature T_S is held at a fixed value (typically between room temperature and liquid-nitrogen or liquid-helium temperature). After deposition, the sample is quenched to a temperature, at which diffusion is entirely frozen and imaged by scanning probe microscopy. This experiment is carried out for different substrate temperatures T_S. For each experiment, the island density of the deposited species is counted and plotted against the substrate temperature T_S at deposition. The slope m of $\ln \hat{N}$ versus T^{-1} determines the diffusion barrier to

$$E_d = k_B \frac{i^*+2}{i^*} m - \frac{E_{i^*}}{i^*} \qquad (3)$$

and the axis intercept $N_0 = \lim_{T_S^{-1} \to 0} \hat{N}$ gives the attempt frequency

$$\nu_0 = 4 F \frac{\Omega^2}{l^2} \left(\frac{0.25}{N_0} \right)^{i^*+2/i^*}. \qquad (4)$$

For obtaining both values, the critical island size i^* must be identified first. This can be done by analyzing the island size distributions, as described in the following section.

B. Island size distribution

We consider the steady-state nucleation regime with an island size distribution n_a (n_a denotes the density of islands with size a). In this case the dynamic scaling hypothesis[46–49] states that n_a scales with the following three parameters: the coverage θ, the mean island size A and a scaling function $f_{i^*}(a/A)$

$$n_a = \theta A^{-2} f_{i^*}(a/A). \qquad (5)$$

The scaling function depends solely on the critical island size and the ratio of a/A but not on the coverage. Based on kinetic Monte Carlo simulations, an empirical function for $f_{i^*}(a/A)$ has been constructed[50]

$$f_{i^*}(a/A) = c_{i^*}(a/A)^{i^*} \exp(-i^* b_{i^*}(a/A)^{1/b_{i^*}}), \qquad (6)$$

where c_{i^*} and b_{i^*} are fixed through the normalization conditions $\int_0^\infty f_{i^*}(a/A) \mathrm{d}(a/A) = \int_0^\infty (a/A) f_{i^*}(a/A) \mathrm{d}(a/A) = 1$.

C. Determining the critical island size

To obtain the critical island size from experiments, the island size distribution n_a is analyzed for different coverages at a fixed temperature and compared to the theoretical island size distributions for different i^* given by Eq. (6).

This was accomplished in a series of molecular adsorption experiments with coverages ranging from $\theta = 0.10$ ML to $\theta = 0.28$ ML performed at a substrate temperature of $T_S = 217$ K. Samples were quenched to 92 K for NC-AFM measurements. Island sizes were determined from topography images, using the threshold marking functionality from GWYDDION. Artifacts were manually removed before exporting the island size distributions. The island sizes may be shifted due to thermal drift, the size of the tip apex and feedback settings. These issues will be discussed in the following. To estimate the maximum error of drift effects, a rather large lateral drift of 0.1 nm/s for the slow scanning direction is assumed. Thus, for typical scanning parameters (frame size 3000 nm × 3000 nm and time 1000 s per frame) the relative error is about 3%.[51] For the error arising from the size of the imaging tip, we assume a typical tip size of 10 nm. This yields a relative error of 0.4% at a frame size of 3000 nm × 3000 nm. Thus, the size of the tip is negligible for the analysis of large frames. Moreover, feedback settings may affect the apparent island size, e.g., with slow feedback settings the islands get elongated on the rear site along the fast scanning direction. In these cases, a comparison of the forward and backward scan clarified the outer shape of the island.

Figure 2 shows the data of the scaled island size distribution $n_a A^2 / \theta$ plotted against the normalized island size a/A for three different coverages. As expected, the scaled data points lie on one smooth curve except for the deviations due to experimental errors. Scaling functions $f_{i^*}(a/A)$ were calculated for $i^* = 1, 2, 3$ according to Eq. (6). Clearly, the experimental data is best described by the model curve for $i^* = 1$ at $T_S = 217$ K. In other words, dimers and all larger clusters are stable at 217 K and are not assumed to decay.

D. Determining the diffusion barrier and attempt frequency

Using the critical island size from the previous section, the diffusion barrier E_d and the attempt frequency ν_0 can now be determined exploiting the dependence of the island density on temperature. This has been accomplished by procedures described in the following.
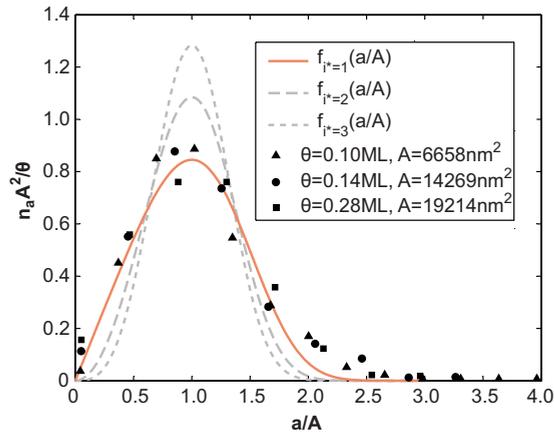
FIG. 2. (Color online) Histogram of the island size distribution for different coverages θ. (Note that each data point represents an interval of island sizes, which is 2174 nm^2, 5731 nm^2, and 7984 nm^2 for the triangles, circles, and squares, respectively.) Upon molecule deposition, the sample temperature was held at T_S =217 K. For measurements, the sample was quenched to 92 K. The maximum relative error is $\pm 8\%$ for the abscissa and $\pm 12\%$ for the ordinate. The error mainly originates from thermal drift issues. Comparison with scaling functions $f_{i^*}(a/A)$ for different i^* gives strong evidence for a critical island size of $i^*=1$.

The sample was prepared with a fixed molecular coverage of $\theta=0.10$ ML at temperatures T_S between 96 and 217 K and quenched to 92 K for NC-AFM measurements. Representative images obtained at several substrate temperatures are compiled in Fig. 3. At each temperature T_S, the island density per adsorption site $\hat{N}$ was determined from the images. The island densities were obtained from a total of 1300
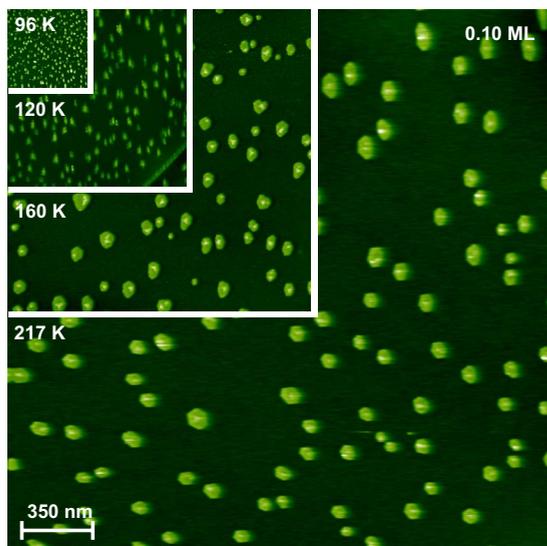
FIG. 3. (Color online) NC-AFM images (topography) at a coverage of $\theta=0.10$ ML at different substrate temperatures between 96 and 217 K. With decreasing temperature, the island density increases and is assumed to follow Eq. (1). Islands are one monolayer high, with an insignificant second layer nucleus (see main text). The scale bare applies to all images.
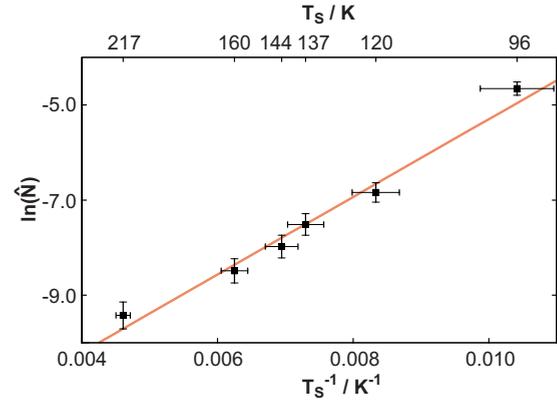
FIG. 4. (Color online) Upon decreasing substrate temperature T_S the island density $\hat{N}$ increases and is assumed to follow Eq. (1). The slope reveals the diffusion barrier to $E_d=(214 \pm 16)$ meV.

islands. We assume an error of $\Delta \hat{N}=4\%$ for the island densities. In Fig. 4, $\ln \hat{N}$ versus T_S^{-1} is plotted and it can be seen that the data points follow a linear dependence. As the critical island size was determined to be $i^*=1$ for 217 K and no distinct variations from the linear dependence are observed for lower temperatures from Fig. 4, we can safely assign i^* =1 for island growth between 96 K and 217 K. From the slope of the linear regression of the data, a diffusion barrier of $E_d=(214 \pm 16)$ meV is derived according to Eq. (3). The attempt frequency $\nu_0=1.4 \times 10^{12 \pm 0.6}$ s^{-1} is taken from the axis intercept according to Eq. (4).

V. CONCLUSION

In summary, we analyzed the diffusion of C_{60} molecules on the atomically flat CaF$_2$(111) surface at various substrate temperatures under the clean conditions of an ultrahigh vacuum. At low temperatures, we observed the coexistence of two domains, with a hexagonal island shape.

For the determination of the diffusion parameters we analyzed island densities and island sizes instead of observing single-molecule hopping events. We determined the critical island size ($i^*=1$) and the diffusion barrier (E_d =(214 $\pm$ 16) meV) for this system.

The value for the diffusion barrier agrees well with the general picture of a weak molecule-substrate interaction in the case of insulating surfaces ($E_d \lesssim 400$ meV).[31–35] It is much lower than the diffusion barrier of C_{60} molecules on metal surfaces, e.g., 1400 meV on Pd(110).[16] Moreover, the attempt frequency $\nu_0 \approx 10^{12}$ s^{-1} lies within the range of previously reported values for large molecules (10^{10} to 10^{14} s^{-1}).[14–16]

The knowledge of the diffusion barrier plays a major role in exploiting molecular arrangements at different temperatures. It is, for example, possible to tune the island density by varying the substrate temperature. Thereby, a specific density of uniformly shaped C_{60} clusters can be created, which is of great importance for future molecular electronics, e.g., for the use as nanopads.[52]

*kuehnle@uni-mainz.de; http://www.uni-mainz.de/FB/Chemie/Kuehnle

[1] C. Joachim, J. K. Gimzewski, and A. Aviram, Nature (London) **408**, 541 (2000).

[2] G. M. Whitesides and B. Grzybowski, Science **295**, 2418 (2002).

[3] J. V. Barth, G. Costantini, and K. Kern, Nature (London) **437**, 671 (2005).

[4] A. Kühnle, Curr. Opin. Colloid Interface Sci. **14**, 157 (2009).

[5] J. V. Barth, Annu. Rev. Phys. Chem. **58**, 375 (2007).

[6] J. V. Barth, Surf. Sci. Rep. **40**, 75 (2000).

[7] T. Michely and J. Krug, *Islands, Mounds and Atoms: Patterns and Processes in Crystal Grwoth Far from Equilibrium* (Springer-Verlag, Berlin, Germany, 2004).

[8] J. A. Venables, *Introduction to Surface and Thin Film Processes* (Cambridge University Press, Cambridge, United Kingdom, 2000).

[9] P. Jensen, Rev. Mod. Phys. **71**, 1695 (1999).

[10] R. Gomer, Rep. Prog. Phys. **53**, 917 (1990).

[11] H. Brune, Surf. Sci. Rep. **31**, 125 (1998).

[12] J. V. Barth, H. Brune, B. Fischer, J. Weckesser, and K. Kern, Phys. Rev. Lett. **84**, 1732 (2000).

[13] J. Krug, Physica A **313**, 47 (2002).

[14] M. Schunack, T. R. Linderoth, F. Rosei, E. Lægsgaard, I. Stensgaard, and F. Besenbacher, Phys. Rev. Lett. **88**, 156102 (2002).

[15] J. Weckesser, J. V. Barth, and K. Kern, J. Chem. Phys. **110**, 5351 (1999).

[16] J. Weckesser, J. V. Barth, and K. Kern, Phys. Rev. B **64**, 161403 (2001).

[17] J. Schütte, R. Bechstein, M. Rohlfing, M. Reichling, and A. Kühnle, Phys. Rev. B **80**, 205421 (2009).

[18] P. A. Gravil, M. Devel, P. Lambin, X. Bouju, C. Girard, and A. A. Lucas, Phys. Rev. B **53**, 1622 (1996).

[19] T. Kunstmann, A. Schlarb, M. Fendrich, T. Wagner, R. Möller, and R. Hoffmann, Phys. Rev. B **71**, 121403 (2005).

[20] S. A. Burke, J. M. Topple, and P. Gruetter, J. Phys.: Condens. Matter **21**, 423101 (2009).

[21] R. Lüthi, E. Meyer, H. Haefke, L. Howald, W. Gutmannsbauer, and H. J. Güntherodt, Science **266**, 1979 (1994).

[22] M. R. Sørensen, K. W. Jacobsen, and H. Jónsson, Phys. Rev. Lett. **77**, 5067 (1996).

[23] M. Bott, M. Hohage, M. Morgenstern, T. Michely, and G. Comsa, Phys. Rev. Lett. **76**, 1304 (1996).

[24] Y. W. Mo, Phys. Rev. Lett. **71**, 2923 (1993).

[25] M. Ternes, C. P. Lutz, C. F. Hirjibehedin, F. J. Giessibl, and A. J. Heinrich, Science **319**, 1066 (2008).

[26] Y. Sugimoto, P. Jelinek, P. Pou, M. Abe, S. Morita, R. Pérez, and O. Custance, Phys. Rev. Lett. **98**, 106104 (2007).

[27] S. Hirth, F. Ostendorf, and M. Reichling, Nanotechnology **17**, S148 (2006).

[28] F. Loske and A. Kühnle, Appl. Phys. Lett. **95**, 043110 (2009).

[29] B. Krause, A. C. Durr, K. Ritley, F. Schreiber, H. Dosch, and D. Smilgies, Phys. Rev. B **66**, 235404 (2002).

[30] B. Müller, T. Kuhlmann, K. Lischka, H. Schwer, R. Resel, and G. Leising, Surf. Sci. **418**, 256 (1998).

[31] B. Stadlober, U. Haas, H. Maresch, and A. Haase, Phys. Rev. B **74**, 165302 (2006).

[32] G. Berlanda, M. Campione, M. Moret, A. Sassella, and A. Borghesi, Phys. Rev. B **69**, 085409 (2004).

[33] R. Ruiz, B. Nickel, N. Koch, L. C. Feldman, R. F. Haglund, A. Kahn, F. Family, and G. Scoles, Phys. Rev. Lett. **91**, 136102 (2003).

[34] M. Tejima, K. Kita, K. Kyuno, and A. Toriumi, Appl. Phys. Lett. **85**, 3746 (2004).

[35] Y. H. Tang, Y. Wang, G. Wang, H. B. Wang, L. X. Wang, and D. H. Yan, J. Phys. Chem. B **108**, 12921 (2004).

[36] A. S. Foster, C. Barth, A. L. Shluger, R. M. Nieminen, and M. Reichling, Phys. Rev. B **66**, 235417 (2002).

[37] L. Tröger, J. Schütte, F. Ostendorf, A. Kühnle, and M. Reichling, Rev. Sci. Instrum. **80**, 063703 (2009).

[38] F. Loske, R. Bechstein, J. Schütte, F. Ostendorf, M. Reichling, and A. Kühnle, Nanotechnology **20**, 065606 (2009).

[39] U. Zerweck, C. Loppacher, T. Otto, S. Grafström, and L. M. Eng, Phys. Rev. B **71**, 125424 (2005).

[40] S. Fölsch, T. Maruno, A. Yamashita, and T. Hayashi, Appl. Phys. Lett. **62**, 2643 (1993).

[41] S. Fölsch, T. Maruno, A. Yamashita, and T. Hayashi, Surf. Sci. **294**, L959 (1993).

[42] D. Walton, J. Chem. Phys. **37**, 2182 (1962).

[43] J. A. Venables, Philos. Mag. **27**, 697 (1973).

[44] J. A. Venables, G. D. T. Spiller, and M. Hanbucken, Rep. Prog. Phys. **47**, 399 (1984).

[45] H. Brune, G. S. Bales, J. Jacobsen, C. Boragno, and K. Kern, Phys. Rev. B **60**, 5991 (1999).

[46] T. Vicsek and F. Family, Phys. Rev. Lett. **52**, 1669 (1984).

[47] F. Family and P. Meakin, Phys. Rev. Lett. **61**, 428 (1988).

[48] M. C. Bartelt and J. W. Evans, Phys. Rev. B **46**, 12675 (1992).

[49] J. G. Amar, F. Family, and P. M. Lam, Phys. Rev. B **50**, 8781 (1994).

[50] J. G. Amar and F. Family, Phys. Rev. Lett. **74**, 2066 (1995).

[51] P. Rahe, R. Bechstein, and A. Kühnle, J. Vac. Sci. Technol. B **28**, C4E31 (2010).

[52] P. Zahl, M. Bammerlin, G. Meyer, and R. R. Schlittler, Rev. Sci. Instrum. **76**, 023707 (2005).